Fast-Photoneutron Spectra due to 55–85-MeV Photons*

N. N. KAUSHAL,† E. J. WINHOLD,§ P. F. YERGIN, H. A. MEDICUS, AND R. H. AUGUSTSON‡
Department of Physics and Astronomy, Rensselaer Polytechnic Institute, Troy, New York 12181
(Received 3 June 1968)

Energy spectra of fast photoneutrons from eighteen elements (Li, Be, B, C, N, O, Al, S, Fe, Cu, Zn, In, Sn, Ta, Tl, Pb, Bi, and U) were measured at 67½°, using thin-target bremsstrahlung from the Rensselaer linac. The neutron detection system utilized a 100-meter flight path and had an over-all time resolution of 0.4 nsec/m. Measurements of the spectra from each target at bremsstrahlung energies of both 55 and 85 MeV permitted extraction of neutron difference spectra effectively due to photons between 55 and 85 MeV. Absolute normalization of the spectra was effected by comparison with the experimentally measured photoneutron spectrum of deuterium. Difference spectra were obtained for neutron energies greater than 10 MeV. Cross sections for production of these neutrons ranged from 59 μb/sr for lithium to 1.28 mb/sr for uranium. The experimental data were compared to the predictions of the quasideuteron model as recently modified by Levinger, with secondary-neutron effects estimated by Monte Carlo calculations. Good agreement was obtained for the absolute-neutron-production cross sections and the shapes of the neutron energy spectra over the range of targets studied.

I. INTRODUCTION

THE high-energy region above the photonuclear giant resonance between 40 MeV and the photopion threshold has remained relatively unexplored in recent years, despite the fact that the integrated photon absorption cross section in this tail region is of comparable magnitude to that in the well-studied giant-resonance region. Some experimental information on the size and shape of the cross section in this region has come from excitation-function studies of (γ,n) reaction cross sections,[1–3] of total-neutron-production cross sections,[4–6] and of reactions involving multiple nucleon emission,[7] but these studies are relatively incomplete. Photoproton spectra from several light elements have also been studied.[8–10] These experiments indicate that direct processes are important and suggest that the quasideuteron model of photon absorption may be applicable to this energy region. This model was first introduced by Levinger[11] to account for photonuclear processes above 200 MeV, and in that region it has successfully predicted production cross sections for high-energy nucleons, energy and angular distributions of the outgoing nucleons, as well as the presence of neutron-proton coincidences.[12] Nevertheless, the detailed nature of the photon absorption process in the tail region remains an open question.

There are no detailed studies of fast-photoneutron spectra in this energy region, yet such experiments should throw considerable light on the character of the

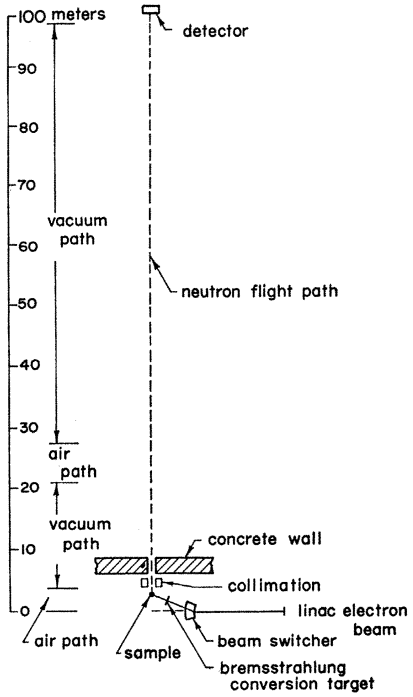

FIG. 1. Over-all experimental arrangement.

* Work supported by the National Science Foundation.
† Present address: Division of Nuclear Engineering and Science, Rensselaer Polytechnic Institute, Troy, N.Y.
§ On leave at Atomic Energy Research Establishment, Harwell, England.
‡ Present address: Los Alamos Scientific Laboratory, Los Alamos, N. M.
[1] B. C. Cook, J. E. E. Baglin, J. N. Bradford, and J. E. Griffin, Phys. Rev. **143**, 712 (1966).
[2] B. C. Cook, J. E. E. Baglin, J. N. Bradford, and J. E. Griffin, Phys. Rev. **143**, 724 (1966).
[3] B. C. Cook, D. R. Hutchinson, R. C. Waring, J. N. Bradford, R. G. Johnson, and J. E. Griffin, Phys. Rev. **143**, 730 (1966).
[4] L. W. Jones and K. M. Terwilliger, Phys. Rev. **91**, 699 (1953).
[5] S. Costa, F. Ferrero, S. Ferroni, B. Minetti, and C. Molino, Phys. Letters **6**, 226 (1963).
[6] S. Costa, F. Ferrero, S. Ferroni, and C. Molino, Phys. Letters **11**, 324 (1964).
[7] See, for example, J. Moffatt and D. Reitman, Nucl. Phys. **65**, 130 (1965).
[8] C. Whitehead, W. R. McMurray, M. J. Aitken, N. Middlemas, and C. H. Collie, Phys. Rev. **110**, 941 (1958).
[9] E. B. Bazhanov, Zh. Eksperim. i Teor. Fiz. **37**, 374 (1959) [English transl.: Soviet Phys.—JETP **10**, 267 (1960)].
[10] J. L. Matthews, W. Bertozzi, S. Kowalski, C. P. Sargent, and W. Turchinetz, Bull. Am. Phys. Soc. **12**, 482 (1967).
[11] J. S. Levinger, Phys. Rev. **84**, 43 (1951).
[12] A. C. Odian, P. C. Stein, A. Wattenberg, B. T. Feld, and R. Weinstein, Phys. Rev. **102**, 837 (1956); M. Q. Barton and J. H. Smith, *ibid.* **110**, 1143 (1958); J. Garvey, B. H. Patrick, J. G. Rutherglen, and I. L. Smith, Nucl. Phys. **70**, 241 (1965).

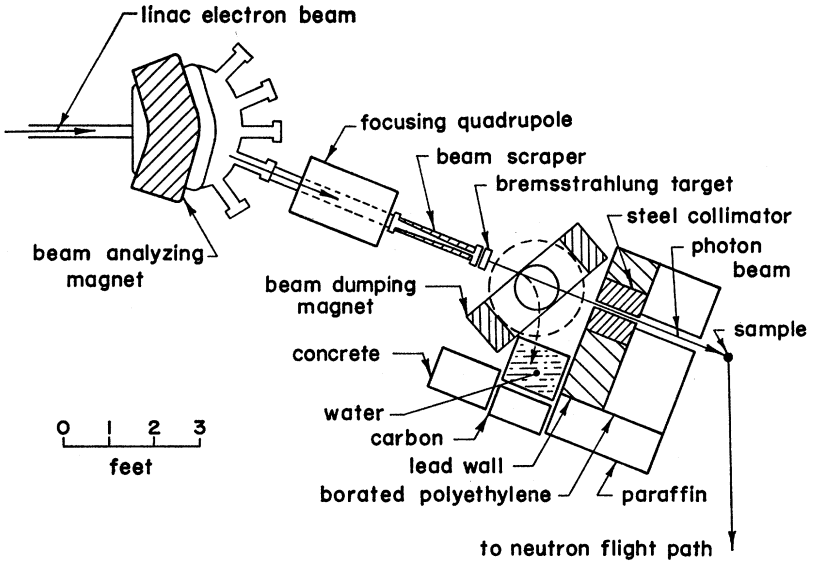

FIG. 2. Beam handling and shielding arrangement in target room.

photon absorption process. In the present experiment neutron time-of-flight techniques have been used to study the energy spectra of fast photoneutrons from a series of 18 elements (ranging in Z from 3 to 92) essentially due to photons between 55 and 85 MeV. While this broad incident photon energy spread undoubtedly masks any detailed features in the emitted neutron spectra, the experiment yields significant information on the systematics of gross spectral shapes and cross-section values as a function of Z.

II. EXPERIMENT

The experimental arrangement is shown in Figs. 1 and 2. The electron beam from the Rensselaer linac is magnetically analyzed and produces thin-target bremsstrahlung when it strikes a 0.010-in.-thick water-cooled tantalum foil. The transmitted electron beam is magnetically deflected and strikes a water beam stopper. The collimated photon beam strikes the target under investigation, which is placed at the intersection of the photon beam axis and the neutron flight path axis. Outgoing photoneutrons from the target that travel down the flight path are emitted at an angle of $67\frac{1}{2}°$ to the incident photon beam. The proton recoil neutron detector is placed at the end of the 100-m flight path. It consists of a liquid-scintillator tank,[13] 5 in. in thickness and 20 in. in diam, viewed by seven Philips 58 AVP photomultipliers.

The photomultipliers are normally biased off, so that they are insensitive to the γ flash associated with each machine pulse. After each pulse they are gated on, starting 0.5 μsec after the arrival of the γ flash, for a period of 14 μsec. A tungsten filter 1 in. thick is placed in the neutron flight path to further reduce the γ-flash effects. Each photomultiplier output drives a low-level fast discriminator circuit. The outputs of these drive an "any three" coincidence circuit whose function is to reduce tube noise background. To minimize machine-dependent background, the discriminators were set at a level corresponding to a threshold energy for neutron detection of about one MeV.

The neutron flight-time measurement utilized a multichannel digital time analyzer with a channel width of 31.25 nsec. The current pulse from the electron beam stopper served as a start pulse and the detector output pulse served as a stop pulse. Over-all system stability was better than one channel. The linac was operated with a beam pulse width of 20 nsec during the experiment. The absolute neutron transit time scale, and hence the absolute neutron energy scale, was obtained by placing a carbon absorber in the neutron flight path and observing the well-known neutron resonance in carbon at 2.076 MeV.[14]

Samples of 18 different elements (Li, Be, B, C, N, O, Al, S, Fe, Cu, Zn, In, Sn, Ta, Tl, Pb, Bi, U) were used. The solid samples were circular disks of $\frac{3}{4}$ in. or 1 in. diam. oriented so that the disk axis coincided with the photon beam axis. Disk thicknesses were $\frac{1}{8}$ in. or $\frac{3}{16}$ in. for heavier nuclei ($Z>20$) and between 1 and 2 in. for lighter elements. Water and liquid nitrogen in thin-walled aluminum containers were used as the samples for the studies of oxygen and nitrogen. Corrections were made for photon attenuation in the samples; these were under 10% in most cases and never exceeded 20%. Approximate corrections were also made for the scattering of the outgoing neutrons in the samples; these corrections amounted to less than 10% in all cases.

Relative photon intensity normalization from run to run was obtained by the use of 1-mil-thick cobalt foils

[13] The scintillator liquid consisted of 7 g/liter p-terphenyl and 0.1 g/liter POPOP (1, 4-bis-(2-(5-(phenyloxazolyl))-benzene) in toluene.

[14] J. E. Wills, Jr., J. K. Bair, H. O. Cohn, and H. B. Willard, Phys. Rev. 109, 891 (1958).

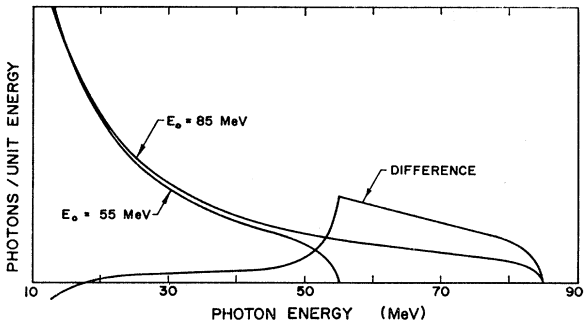

FIG. 3. Bremsstrahlung spectra with 55- and 85-MeV endpoints together with the corresponding difference spectrum (× 2). The two spectra are here normalized for equal photon numbers at 18 MeV.

of the same diameter as the sample. One of these foils was attached to the sample during each run. The intensity of the 810-keV Fe^{58} γ ray associated with the 71.6-day Co^{58} activity was subsequently counted for each foil. This activity is a measure of the $Co^{59}(\gamma,n)$ yield in the foil. The $Co^{59}(\gamma,n)$ cross section is known[15] to rise from threshold near 10 MeV to the giant-resonance peak at about 18 MeV and then fall off and effectively reach zero by 26 MeV. Hence, normalization of the photoneutron yields to unit cobalt activity corresponds to normalization for equal numbers of photons in the vicinity of 18 MeV.

Runs were made on each sample at bremsstrahlung endpoint energies of 55 and 85 MeV. The neutron yields from both these runs were normalized, on the basis of cobalt monitor foil activity, for equal numbers of photons at the giant-resonance peak energy for the sample. The neutron spectrum obtained at 55 MeV was then subtracted from the 85-MeV neutron spectrum. The resultant neutron difference spectrum is thus primarily due to photons between 55 and 85 MeV. The photon difference spectrum is the difference between the 85- and 55-MeV bremsstrahlung spectra, as indicated in Fig. 3; this spectrum has a low-energy tail extending below 55 MeV in addition to the main photon slice between 55 and 85 MeV.

The observed neutron spectra must be corrected for the variation of detector efficiency with neutron energy. This was experimentally determined by measuring the photoneutron spectrum from deuterium. In this case the disintegration cross section is experimentally known; moreover, because of the two-body breakup there is a one to one relation between the neutron energy E_n and the photon energy E_γ. Runs were made at an electron energy of 85 MeV on targets of both ordinary and heavy water under identical conditions. The spectra from the two runs were normalized per unit cobalt activity and the ordinary-water spectrum was subtracted from the heavy-water spectrum to remove the oxygen photoneutron contribution and yield a neutron spectrum $N_D(E_n)$ due only to deuterium. The detector efficiency $\epsilon(E_n)$ is given by

$$\epsilon(E_n)=\frac{CN_D(E_n)}{K_D(E_\gamma,E_0)(d\sigma/d\omega)_D(E_\gamma)n_D}\left(\frac{dE_n}{dE_\gamma}\right)_D^{-1}, \quad (1)$$

where $N_D(E_n)$ is the normalized number of deuterium photoneutrons detected per MeV at energy E_n, $K_D(E_\gamma,E_0)$ is the number of bremsstrahlung photons per MeV at energy E_γ incident on the deuterium sample per unit cobalt activity (E_0 is the endpoint energy), $d\sigma/d\omega$ is the differential cross section for photoneutron emission from deuterium at $67\frac{1}{2}°$ in the laboratory, n_D is the number of deuterium target nuclei, $(dE_n/dE_\gamma)_D \simeq \frac{1}{2}$, and C is a constant dependent on the experimental geometry. The Schiff thin-target spectrum was used for K and the deuterium cross section was obtained from the calculations of Partovi,[16] which are in good agreement with available experimental data. The relative efficiency determined in this manner is shown in Fig. 4. Useful efficiency data is obtained only out to a neutron energy of 35 MeV. Beyond this energy the efficiency curve has been smoothly extrapolated in a manner consistent with detector efficiency calculations[17] and with other experimental efficiency determinations on similar detectors of this size.[18]

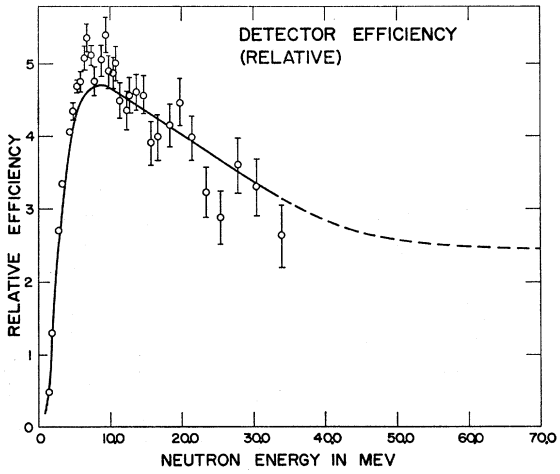

FIG. 4. Relative detector efficiency as a function of neutron energy.

Comparison with the deuterium photoneutron spectrum measurement also permits extraction of absolute photoneutron yields. The observed neutron spectrum in a given run using bremsstrahlung of end-point E_0 is equal to

$$N_s(E_n,E_0)=n_s\epsilon(E_n)Y_s(E_n,E_0)/C, \quad (2)$$

where N_s is the normalized number of neutrons per

[15] S. C. Fultz, R. L. Bramblett, J. T. Caldwell, N. E. Hansen, and C. P. Jupiter, Phys. Rev. 128, 2345 (1962).

[16] F. Partovi, Ann. Phys. (N. Y.) 27, 79 (1964).

[17] R. J. Kurz, University of California Radiation Laboratory Report No. UCRL-11339, 1964 (unpublished).

[18] C. E. Wiegand, T. Elioff, W. B. Johnson, L. B. Auerbach, J. Lach, and T. Ypsilantis, Rev. Sci. Instr. 33, 526 (1962).

MeV at energy E_n detected from the sample, n_s is the number of target nuclei, ϵ is the detector efficiency given by (1) in terms of the deuterium experiment, C is the same constant as in (1), and the yield Y_s is given by

$$Y_s(E_n,E_0)=\int_0^{E_0}\frac{d^2\sigma}{dE_n d\omega}(E_n,E_\gamma)K(E_\gamma,E_0)dE_\gamma. \quad (3)$$

The absolute yield of the neutron difference spectrum due to the 85–55-MeV photon difference spectrum can be specified in terms of an effective cross section $(d^2\sigma/dE_n d\omega)_{\text{eff}}$ for production of neutrons of energy E_n by photons in the difference spectrum, which is given by

$$[d^2\sigma/dE_n d\omega(E_n)]_{\text{eff}}$$
$$=\frac{[Y_s(E_n,85)-Y_s(E_n,55)]}{\int^{85}[K(E_\gamma,85)-K(E_\gamma,55)]dE_\gamma}$$
$$=\frac{2n_D[N_s(E_n,85)-N_s(E_n,55)]K_D(E_\gamma,E_0)(d\sigma/d\omega)_D}{n_s N_D(E_n)\int^{85}[K(E_\gamma,85)-K(E_\gamma,55)]dE_\gamma}. \quad (4)$$

In the actual extraction of these effective cross sections

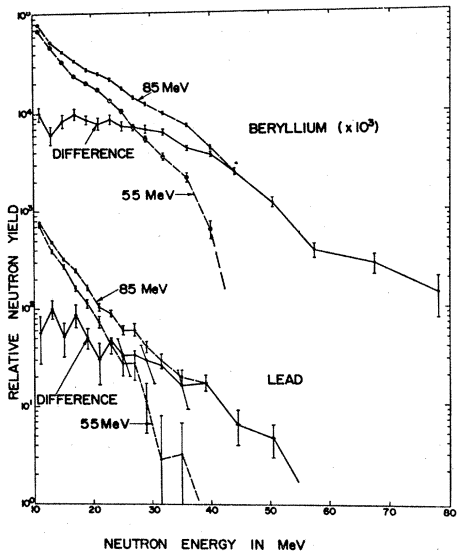

FIG. 5. Neutron energy spectra for beryllium and lead due to 55- and 85-MeV bremsstrahlung, together with the corresponding difference neutron spectra. Error bars indicate statistical errors only.

from the data, no account was taken of the low-energy tail in the photon difference spectrum, shown in Fig. 3.

III. RESULTS

The experimental spectra at 55 and 85 MeV for beryllium and lead are shown in Fig. 5, together with the corresponding difference spectra. The spectra for these two nuclei are reasonably typical of those for light and heavy nuclides, respectively. Although data were taken down to a neutron energy of 2 MeV, the spectra are plotted only down to 10 MeV. Below this neutron energy the photoneutron yields from the individual runs at 55 and 85 MeV become very large with small fractional differences so that the differences have very large statistical uncertainties. The data of Fig. 5 also illustrate the result that the fractional difference for the heavy nuclei is smaller than for the light nuclei, especially at lower neutron energies, so that the difference-spectra statistics are in general better for the light nuclei than for the heavy.

The difference spectra for all 18 target nuclei are plotted together on the same absolute cross-section scale in Fig. 6. In the case of nitrogen, reliable difference data were obtained only down to 25 MeV because of uncertainties in photon intensity normalization in those runs.

IV. DISCUSSION

Several general features of the difference spectra are evident.

(1) A sizeable yield of fast neutrons above 10 MeV is present in all the spectra. These high-energy neutrons must arise from a relatively direct interaction between photon and emitted neutron.

(2) The light element spectra are similar in general shape, falling off approximately linearly from 30 MeV to zero at about 55 MeV. These similarities occur in spite of the large variation in particle separation energies from nucleus to nucleus.

(3) There is a definite trend in shape from the light to heavy nuclei. The spectra due to the light elements

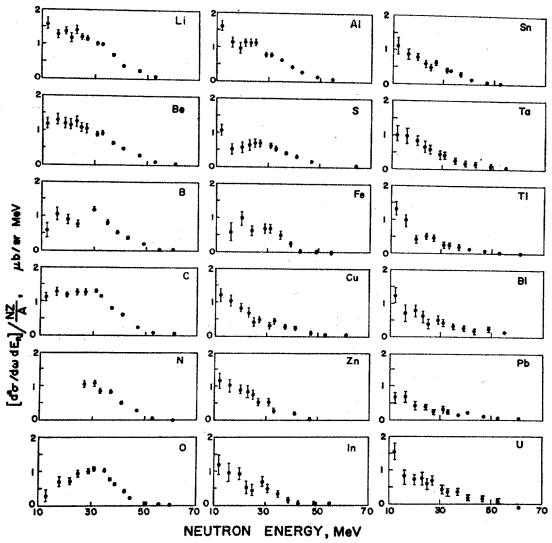

FIG. 6. Observed neutron spectra due to 55–85-MeV difference photon spectra. The effective cross sections have been divided by NZ/A.

TABLE I. Comparison of present cross-section values in mb for production of high-energy photoneutrons by 55–85-MeV photons with measured cross sections $\sigma(\gamma,Tn)$, also in mb, for total photoneutron production. The present cross-section values are uncertain by 8 to 10% because of counting statistics and normalization errors; in addition all values depend on an absolute normalization in terms of the deuteron photodisintegration cross section, which is known to about 10% at these energies.

Target	$4\pi(d\sigma/d\omega)_{67}°$ ($E_n>10$ MeV) [Present experiment]	$\sigma(\gamma,Tn)$ Jones and Terwilliger[a]	Costa *et al.*[b]	Other results
Li	0.75		1.0	
Be	1.0	2.7	2.3	2.3[c]
B	1.0		1.4	
C	1.5	1.3	1.4	2.4[d]
O	1.3		1.6	
Al	2.8	5.5	4.6	8[d]
S	2.1		4.4	6.5[d]
Fe	4.2	16	12	
Cu	4.3	20	19	
Zn	4.4		15	
In	7.4			
Sn	7.0			
Ta	10.7	95		
Tl	10.7			
Pb	8.3	100		
Bi	13			
U	16	65		

[a] Average cross sections between 55 and 85 MeV, as read from Figs. 4 and 5 of Ref. 4.
[b] $\int_0^{80}\sigma dE-\int_0^{30}\sigma dE/50$, as taken from Fig. 4 of Ref. 5 and Table I of Ref. 6.
[c] S. Costa, L. Pasqualini, G. Piragino, and L. Roasio, Nuovo Cimento 42, 306 (1966).
[d] G. Bishop, S. Costa, S. Ferroni, R. Malvano, and G. Ricco, Nuovo Cimento 42, 148 (1966).

are relatively richer in high-energy neutrons (>30 MeV) than those for the heavy elements.

(4) A comparison of our measured cross sections for emission of neutrons with energies >10 MeV with the experimental total-neutron-production cross sections[4–6] at these photon energies is shown in Table I. In the absence of detailed information on the angular distribution of fast photoneutrons in this energy range, our measured differential cross sections at $67\frac{1}{2}°$ have been multiplied by 4π to make this comparison. Available experimental information[19] does suggest that this procedure is satisfactory for the present purpose of comparing cross-section trends. For the light elements ($Z\leq 8$), the present values agree fairly well with the total-neutron-production cross sections. For the heavy elements ($Z\geq 73$) the cross sections for $E_n>10$ MeV are about 10 mb, while the total-neutron-production cross sections are of the order of 100 mb. This implies that most of the neutrons emitted from the heavy elements have energies less than 10 MeV. Thus, there is a general trend from the light elements, where most of the emitted neutrons have energies >10 MeV, to the heavy elements, which have a sizeable evaporation component below 10 MeV.

It is clear from the present results that emission of high-energy neutrons is an important process at photon energies between 55 and 85 MeV. Hence the primary photon-nucleus interaction at these energies frequently involves transfer of a sizeable fraction of the photon energy to a single nucleon. However, the detailed character of the photon absorption process in this energy region is still an open question.

Direct photoelectric absorption of a photon by a single nucleon has been considered by several authors as the mechanism for the emission of high-energy nucleons in this energy region. Fujii[20] has calculated on this basis, cross sections for (γ,p) transitions to low-lying states in light nuclei, using square-well shell-model wave functions, and his results are in reasonable agreement with available experimental data. Shklyarevskii[21] on the other hand, made similar calculations for $C^{12}(\gamma,p)$ using oscillator wave functions and found that the calculated cross section was too small and fell off much too fast with increasing photon energy in the tail region. This latter result is consistent with the idea that the single-particle model cannot provide the needed high momentum of the outgoing nucleon since the incoming photon momentum is small and the single-particle states in the target should not have high-momentum components.

Shklyarevskii[21] found that inclusion of pair correlations in his single-particle calculation of the $C^{12}(\gamma,p)$ ground-state cross section increased the cross section value substantially and brought it into agreement with experiment. This result suggests that Levinger's quasideuteron model, which was introduced to explain photoabsorption processes above 200 MeV, may also be applicable at energies below 100 MeV. The presence of large numbers of lower-energy non-ground-state fast neutrons observed in the present experiment, which cannot be accounted for by the simple single-particle models, also suggests that the quasideuteron model may be relevant here.

The quasideuteron model assumes that the photon absorption process involves the photodissociation of an interacting neutron-proton pair within the nucleus. In this model the high momenta of the outgoing particles arise from the high-momentum states associated with the closely correlated neutron-proton pairs. Levinger[11] showed that the absorption cross section could be written in the simple form

$$\sigma=(kNZ/A)\sigma_D, \tag{5}$$

where σ_D is the photodisintegration cross section for the free deuteron, and the constant $k\simeq 8$. The validity of this model has been demonstrated experimentally at photon energies above 200 MeV; it successfully predicts cross sections for fast nucleon emission, emitted

[19] G. C. Reinhardt and W. D. Whitehead, Nucl. Phys. **30**, 201 (1962); C. Glavina, J. A. Rawlins, S. H. Ku, L. K. TerVeld, and Y. M. Shin, Bull. Am. Phys. Soc. **12**, 651 (1967).

[20] S. Fujii, Progr. Theoret. Phys. (Kyoto) **29**, 374 (1963).

[21] G. M. Shklyarevskii, Zh. Eksperim. i Teor. Fiz. **41**, 451 (1961) [English transl.: Soviet Phys.—JETP **14**, 324 (1962)].

nucleon energy and angular distributions, and the angular correlations of coincident neutron-proton pairs.

The experimental evidence for the quasideuteron model at photon energies below 100 MeV is considerably more ambiguous than at higher energies. Johansson[22] was unsuccessful in his search for correlated neutron-proton pairs from C^{12} using 65-MeV bremsstrahlung, though this negative result could have been due to the intranuclear scattering of the emerging nucleons. On the other hand, Whitehead *et al.*[8] studied photoproton spectra and angular distributions from several light elements, and concluded that quasideuteron interactions could well account for major contributions to the observed cross sections.

Levinger[23] has recently proposed a modification of the quasideuteron model for the region below 100 MeV. He introduces a damping factor $\exp(-D/E_\gamma)$ into the cross section expression (5) to take account of the reduction in the quasideuteron process at low energies due to the healing of the two-nucleon correlations at large internucleon separations. A choice of $D=30$ MeV yields a cross section for quasideuteron absorption, which exhausts the expected integrated cross section in the tail up to the photopion threshold. Moreover this value of D is reasonably consistent with other information on healing distances.

A comparison of the present data with the predictions of Levinger's modified quasideuteron model is complicated by the interaction of outgoing primary neutrons with the rest of the nucleus, resulting in the possibility of their absorption and of the emission of lower-energy secondary particles and a low-energy evaporation component. These effects are particularly severe for intermediate- and heavy-target nuclei. As a first step in this comparison, the quasideuteron cross-section prediction can be modified to yield the cross section for direct emission of primary nucleons. The probability of emission of an outgoing neutron without further interaction was calculated on the basis of the optical model assuming a uniform distribution of source points and using a volume imaginary potential W derived from optical-model fits[24] to elastic proton scattering data in this energy range. The comparison of this calculation with the cross-section data is shown in Fig. 7. The curve for the quasideuteron cross section with optical attenuation included, has the same A dependence as the experimental data though it is slightly lower in absolute magnitude than the experimental cross section for production of neutrons with energies above 10 MeV.

It is clear that the model reproduces the general trend of the cross-section data. However, it only includes directly emitted primary neutrons, and a more detailed comparison requires that we take account of

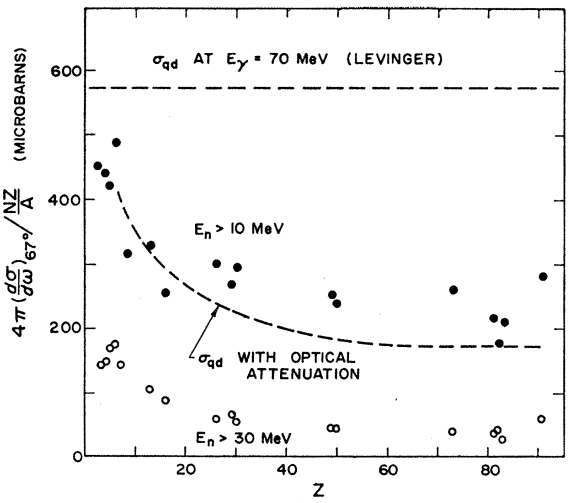

FIG. 7. Effective cross sections for production of fast neutrons with energies greater than 10 MeV (solid circles) and 30 MeV (open circles) by the 55–85-MeV photon difference spectrum. The dashed curves are modified quasideuteron model predictions as discussed in the text.

the emitted secondary neutrons with energies greater than 10 MeV. Both the shapes of the experimental energy spectra and the measured absolute cross sections for neutron production are affected by these secondary neutrons. These effects were estimated for the cases of aluminum and lead by making Monte Carlo calculations of the type first performed by Goldberger.[25]

A high-energy nucleon was assumed to originate at a random position in the nucleus, which was treated as a Fermi gas. Collisions were made at random and all particles were followed till they were absorbed or escaped. Allowable collisions satisfying the Pauli principle were those for which the final energies of both particles were above the Fermi energy. The mean free path used was adjusted to give attenuation consistent with the optical calculation mentioned above. Calculations were made for 20- and 40-MeV particles in aluminum and lead.

The quasideuteron model predictions can now be modified by the results of the above Monte Carlo calculations and compared with the experimental spectrum shapes and absolute-neutron-production cross sections. Dedrick's quasideuteron calculation[26] was used for the primary neutron spectrum. The results are shown in Fig. 8 for beryllium, aluminum, and lead. No corrections for secondary neutrons were considered necessary for beryllium. In all three cases the calculated spectra were arbitrarily multiplied by the same normalizing factor of 1.15 in order to obtain a better over-all fit to the experimental data. The shapes and magnitudes of the observed spectra are well reproduced by the calculations. In particular the smooth increase with A in the relative number of lower-energy neutrons is well

[22] S. A. E. Johansson, Phys. Rev. **97**, 434 (1955).
[23] J. S. Levinger, in *Proceedings of International Conference on Low and Intermediate Energy Electromagnetic Interactions*, (Academy of Sciences, USSR, Moscow, 1967), Vol. 3, p. 411.
[24] R. C. Barrett, A. D. Hill, and P. E. Hodgson, Nucl. Phys. **62**, 133 (1965).
[25] M. L. Goldberger, Phys. Rev. **74**, 1269 (1948).
[26] K. G. Dedrick, Phys. Rev. **100**, 58 (1955).

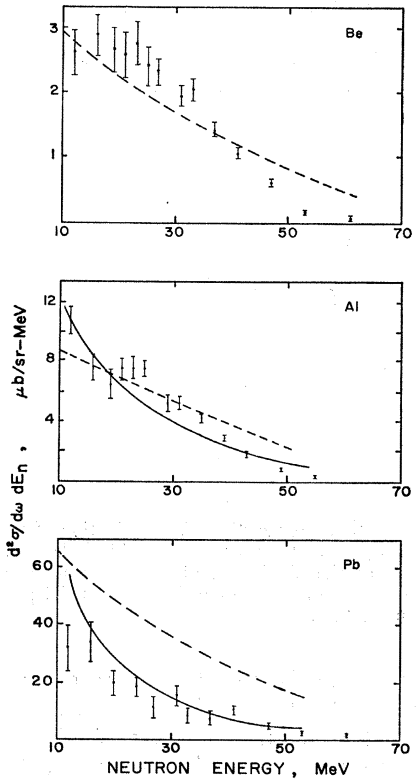

FIG. 8. Neutron energy spectra for beryllium, aluminum, and lead. The dashed curves are Dedrick's quasideuteron model calculations of the primary neutron spectra, arbitrarily multiplied by 1.15. For aluminum and lead these have been modified by estimates of the effects of secondary interactions on the outgoing neutrons, as discussed in the text, to produce the solid curves.

reproduced by the model, which ascribes this increase to the increase with A of the numbers of secondary neutrons.

To summarize, there is remarkably good agreement between the experimental data and the quasideuteron predictions as regards absolute cross sections for fast neutron emission as well as A dependence of the cross sections and neutron energy spectra shapes. The agreement is especially remarkable since the quasideuteron model used is undoubtedly an oversimplification, particularly at photon energies below 100 MeV. In the case of heavy nuclei, where only the outer shells can contribute fast outgoing neutrons at these photon energies, Eq. (5) probably overestimates the number of effective neutron-proton pairs. For light nuclei, attempts[27–29] to refine the quasideuteron model in terms of including two-nucleon correlations in a shell-model framework have not been successful in reproducing experimental cross sections, though they indicate that these are more sensitive to the final-state than to the initial-state correlations. It may be that the simple model, which relates the quasideuteron process directly to free deuteron photodisintegration, implicitly takes into account in this fashion the interaction and the initial- and final-state correlations in a more correct way than do the more elaborate calculations that attempt to include these effects explicitly. While the over-all agreement between the predictions of the simple model and the present experiment does appear to lend support to the basic correctness of the model in this energy range, it is clear that further experimental studies are needed to clarify the nature of the reaction mechanism. In addition, more detailed and more complete theoretical treatments are also clearly needed if there is to be any hope of proceeding to a better understanding of the processes involved. It should be reiterated that the intent of the present experiment was to study with relatively coarse resolution the systematics of high-energy neutron emission, using a relatively broad incident photon energy spread. More detailed studies require finer incident photon energy resolution and should probably concentrate on light nuclei, where secondary neutron effects are less severe and where there is hope for a more refined theoretical treatment.

ACKNOWLEDGMENT

We thank Dr. J. S. Levinger for a series of helpful discussions.

[27] A. Reitan, Nucl. Phys. **36**, 56 (1962).
[28] T. I. Kopaleishvili and R. I. Jibuti, Nucl. Phys. **44**, 34 (1963).
[29] E. Østgaard, Nucl. Phys. **64**, 289 (1965).